

ELECTRICAL CONDUCTIVITY AND MAGNETIC ORDER IN THE SINGLE-BAND HUBBARD MODEL*

W. BORGIEL^a, T. HERRMANN^b, W. NOLTING^b
AND R. KOSIMOW^a^aInstitute of Physics, Silesian University
Uniwersytecka 4, 40-007 Katowice, Poland^bHumboldt-Universität zu Berlin, Institut für Physik
Invalidenstrasse 110, 10115 Berlin, Germany*(Received October 28, 2000)*

A Modified Alloy Analogy (MAA) for the single-band Hubbard model is used to investigate the interplay of ferromagnetic order and electrical conductivity in a system of itinerant band electrons. The alloy analogy is evaluated within the framework of the Coherent Potential Approximation (CPA). The tensor conductivity, normally a two-particle Green function, can be represented by single-particle terms if CPA-consistent approaches are applied [B.Velický, *Phys. Rev.* **184**, 614 (1969)]. The MAA is used for fcc and bcc lattices. Spontaneous ferromagnetism appears in the fcc lattice for a more than half-filled energy band ($1 < n < 2$). In the bcc lattice collective order is restricted to a small n -region. The electrical conductivity is investigated for different Coulomb strengths U as function of band occupation n and temperature T . The conductivity turns out to be substantially higher in the ferromagnetic than in the paramagnetic phase, even diverging in the case of ferromagnetic saturation ($T \rightarrow 0$), where electron-electron scattering is excluded. Majority-spin carriers contribute the main part to the current in the ferromagnetic phase. The electrical resistivity exhibits a power-like low-temperature behavior becoming critical at T_C . Formal similarity to the spin disorder resistivity of local moment systems is observed.

PACS numbers: 75.10.Lp, 71.27.+a, 72.15.-v, 72.15.Eb

* Presented at the XXIV International School of Theoretical Physics "Transport Phenomena from Quantum to Classical Regimes", Ustroń, Poland, September 25–October 1, 2000.

1. Introduction

The electrical conductivity in magnetic materials may be classified into two categories that divides such materials into two classes. The first contains all those substances, in which different groups of electrons are responsible for the electrical current and for the magnetism. Prototypes are the magnetic rare earth elements and certain of their compounds such as Gd and GdS, GdTe. Materials, in which both phenomena are carried by the same electrons, belong to the second category. In the following we focus our considerations on this class of magnetic materials.

We assume charge carriers moving in a narrow energy band with an on-site Coulomb interaction U , only. Restricting the considerations furthermore to a single s -band, so that a lattice site can be occupied at most by two electrons of opposite spins, the highly idealized situation is exactly fitted by the Hubbard model [1–3]. Being one of the simplest but non-trivial models it describes correlated electrons on a lattice. Correlations among itinerant electrons have proven to be responsible for various interesting phenomena like spontaneous magnetic order, the metal-insulator Hubbard–Mott transition as well as probably the high-temperature superconductivity.

Since a long time it has been a challenging task to derive transport properties, in particular the electrical conductivity, within the framework of the single-band Hubbard model [4–16]. In spite of its simple structure the Hubbard Hamiltonian provokes a highly sophisticated many-body problem. It is impossible up to now to formulate for the general case the exact single-electron properties. Approximations must be tolerated. Two-particle Green functions additionally required for the investigation of transport properties are even more difficult to achieve. Within the Hubbard model only very few special cases can be treated rigorously. Bari *et al.* [4] have calculated the conductivity by means of linear response executing all averaging processes in the atomic limit, only. Kubo [17] uses as a starting point the well-known Kubo formula [18] by which the conductivity is expressed by a two-particle Green function. The first equation of motion of that function is decoupled in strict conformity with the procedure introduced by Hubbard [1] for the single-electron Green function (“Hubbard-I-solution”). However, ferromagnetism is possible within this approach only for rather exotic densities of states. The reaction of the conductivity on magnetic phase transitions is, therefore, not disputable. Kikoin and Flerov [19] arrive with a different Green function decoupling procedure at essentially the same conductivity expression as given by Kubo [17]. Bari and Kaplan [5] investigate the interesting limiting case: $\lim_{W \rightarrow 0} \sigma/W^2$, where W is Bloch bandwidth. While the conductivity σ naturally vanishes in the zero-bandwidth limit, σ/W^2 remains finite and can be calculated exactly.

In the recent past, great progress has been achieved in the understanding of the Hubbard model mainly due to the study of the limit of infinite spatial dimensions [20,21], where the Hubbard model can be mapped onto a single-impurity Anderson model [22,23] for which numerically exact solutions can be found by quantum Monte-Carlo calculations. To find an analytical, of course, approximate solution for the electronic selfenergy may be useful, on the other hand, for the derivation of the electrical conductivity, too, if it is possible to express the conductivity by single-particle functions. Velický [24] was the first who demonstrated that this can be realized for the alloy problem treated within the CPA [25].

In this paper we combine the recently developed MAA [26] of the Hubbard model with the CPA-consistent Velický theory for the electrical conductivity [24]. In Sec. 2 we prepare the problem. The Hubbard model and its many-body problem are introduced. Sec. 3 introduces the electrical conductivity along the line pre-described by Velický [24]. The details of the MAA [26] vital for the following discussion are presented in Sec. 4. Sec. 5 illustrates our proposals for the interplay of spontaneous ferromagnetic order and the electrical conductivity within the framework of the Hubbard model. The results are gathered in Sec. 6.

2. Hubbard model

The Hubbard–Hamiltonian represents the simplest starting point for the investigation of correlated fermion systems. Kinetic energy, Coulomb interaction, Pauli principle and lattice structure must be considered the minimum set of terms, the interplay of which determines the electric and magnetic properties

$$\mathcal{H} = \sum_{i,j,\sigma} (T_{ij} - \mu\delta_{ij}) c_{i\sigma}^\dagger c_{j\sigma} + \frac{1}{2}U \sum_{i,\sigma} n_{i\sigma} n_{i-\sigma}. \quad (1)$$

The model assumes that the phenomena to be described are caused by a strongly screened Coulomb interaction being therefore restricted to its intraatomic part only. Itinerant electrons are moving in a non-degenerate s -band. Electrons which meet at the same lattice site \mathbf{R}_i to perform a Coulomb interaction must, therefore, have opposite spins. $n_{i\sigma} = c_{i\sigma}^\dagger c_{i\sigma}$ is the occupation number operator, $c_{i\sigma}^\dagger$ ($c_{i\sigma}$) the creation (annihilation) operator of an electron with spin σ at site \mathbf{R}_i . μ denotes the chemical potential. T_{ij} represent the Fourier transforms of the Bloch energies $\varepsilon(\mathbf{k})$. Model parameters are the effective Coulomb coupling U/W , where W is width of the “free” Bloch band, the band occupation $n = \sum_\sigma \langle n_\sigma \rangle$ ($0 \leq n \leq 2$) and the lattice structure.

The Hubbard–Hamiltonian provokes a non-trivial many-body problem being considered as solved as soon as the single-electron Green function is found:

$$G_{ij\sigma}(E) = \frac{1}{N} \sum_{\mathbf{k}} e^{i\mathbf{k}(\mathbf{R}_i - \mathbf{R}_j)} G_{\mathbf{k}\sigma}(E), \quad (2)$$

$$G_{\mathbf{k}\sigma}(E) = -i \int_0^{\infty} d(t-t') e^{\frac{i}{\hbar} E(t-t')} \left\langle \left[c_{\mathbf{k}\sigma}(t), c_{\mathbf{k}\sigma}^{\dagger}(t') \right]_+ \right\rangle. \quad (3)$$

$\langle \dots \rangle$ stands for the thermodynamic average and $[\dots, \dots]_+$ is the anticommutator. By use of the (complex) electronic selfenergy

$$\Sigma_{\mathbf{k}\sigma}(E) \equiv R_{\mathbf{k}\sigma}(E) + iI_{\mathbf{k}\sigma}(E), \quad (4)$$

a formal solution for the Green function reads as follows:

$$G_{\mathbf{k}\sigma}(E) = \hbar \left[E + \mu - \varepsilon(\mathbf{k}) - \Sigma_{\mathbf{k}\sigma}(E) \right]^{-1}. \quad (5)$$

The Green function is not directly observable but the spectral density $S_{\mathbf{k}\sigma}(E)$

$$S_{\mathbf{k}\sigma}(E) = -\frac{1}{\pi} \text{Im} G_{\mathbf{k}\sigma}(E) = -\frac{\hbar}{\pi} \frac{I_{\mathbf{k}\sigma}(E)}{(E + \mu - \varepsilon(\mathbf{k}) - R_{\mathbf{k}\sigma}(E))^2 + I_{\mathbf{k}\sigma}^2(E)}, \quad (6)$$

which except for transition matrix elements represents the bare lineshape of an angle and spin resolved (direct, inverse) photoemission experiment. An additional wave-vector summation yields the Quasiparticle Density Of States (QDOS):

$$\rho_{\sigma}(E) = \frac{1}{N\hbar} \sum_{\mathbf{k}} S_{\mathbf{k}\sigma}(E - \mu). \quad (7)$$

All single-particle properties, we are interested in, can be derived from the Green function (5). However, this function cannot rigorously be calculated for the Hubbard model. Nevertheless some exact limiting cases are known which, suitably composed, may help to find a reliable approach for the general case.

Very simple but not unimportant is the zero bandwidth limit

$$W \longrightarrow 0; \quad T_{ij} \longrightarrow T_0 \delta_{ij}; \quad \varepsilon(\mathbf{k}) \longrightarrow T_0; \quad \forall \mathbf{k} \quad (8)$$

realized, *e.g.*, by a diverging lattice constant. The energy band is reduced to an N -fold degenerate Bloch level T_0 . A straightforward calculation yields a spectral density (6) consisting of two δ -functions at the quasiparticle levels

T_0 and $T_0 + U$ with spectral weights $\alpha_{1\sigma} = 1 - \langle n_{-\sigma} \rangle$ and $\alpha_{1\sigma} = \langle n_{-\sigma} \rangle$, respectively. $\langle n_{\sigma} \rangle$ is the spin-dependent average occupation number

$$\langle n_{\sigma} \rangle = \int_{-\infty}^{+\infty} dE f_{-}(E) \rho_{\sigma}(E), \quad (9)$$

where

$$f_{-}(E) = (\exp(\beta(E - \mu)) + 1)^{-1}$$

is the Fermi function. Here and in what follows we assume translational symmetry restricting ourselves to paramagnetic and ferromagnetic systems, only. The spectral weights as well as the respective selfenergy [1]

$$\Sigma_{\sigma}^{(0)}(E) = U \langle n_{-\sigma} \rangle \frac{E + \mu - T_0}{E + \mu - T_0 - U(1 - \langle n_{-\sigma} \rangle)}, \quad (10)$$

are determined by $\langle n_{-\sigma} \rangle$ being therefore, at least in principle, particle number-, temperature- and spin-dependent. The selfconsistent evaluation in the zero bandwidth limit, however, yields $\langle n_{-\sigma} \rangle = (1/2)n$, preventing therewith spontaneous magnetism for this special case.

In the case of finite electron hopping but still restricted to the strong coupling regime ($W \ll U$) the spectral density consists of two main peaks, which evolve from the two quasiparticle levels in the $W \rightarrow 0$ limit [27]. In addition satellite peaks appear due to higher order processes which are connected to changes in the number of double occupancies in the system. The spectral weights of these satellites are at most of order $(W/U)^4$ so that the higher-order processes are certainly negligible in the strong coupling regime. The detailed structure of the two main peaks is not known but their spectral weights

$$\alpha_{1\sigma}(\mathbf{k}) = 1 - \alpha_{2\sigma}(\mathbf{k}) \approx 1 - \langle n_{-\sigma} \rangle, \quad (11)$$

as well as their centers of gravity [27]:

$$T_{1\sigma}(\mathbf{k}) \approx (1 - \langle n_{-\sigma} \rangle)\varepsilon(\mathbf{k}) + \langle n_{-\sigma} \rangle B_{\mathbf{k}-\sigma}, \quad (12)$$

$$T_{2\sigma}(\mathbf{k}) \approx U + \langle n_{-\sigma} \rangle \varepsilon(\mathbf{k}) + (1 - \langle n_{-\sigma} \rangle) B_{\mathbf{k}-\sigma}. \quad (13)$$

$B_{\mathbf{k}-\sigma}$ is a ‘‘higher’’ correlation function,

$$B_{\mathbf{k}-\sigma} = B_{-\sigma} + b_{\mathbf{k}-\sigma}, \quad (14)$$

consisting of a local term

$$B_{-\sigma} - T_0 = \frac{1}{\langle n_{-\sigma} \rangle (1 - \langle n_{-\sigma} \rangle)} \frac{1}{N} \sum_{i,j}^{i \neq j} T_{ij} \langle c_{i-\sigma}^{\dagger} c_{j-\sigma} (2n_{i\sigma} - 1) \rangle, \quad (15)$$

and a \mathbf{k} -dependent part:

$$b_{\mathbf{k}-\sigma} = \frac{1}{\langle n_{-\sigma} \rangle (1 - \langle n_{-\sigma} \rangle)} \frac{1}{N} \sum_{i,j}^{i \neq j} T_{ij} e^{-i\mathbf{k} \cdot (\mathbf{R}_i - \mathbf{R}_j)} \\ \times \left\{ \langle n_{i-\sigma} n_{j-\sigma} \rangle \langle n_{-\sigma} \rangle^2 + \langle c_{j-\sigma}^\dagger c_{j\sigma}^\dagger c_{i-\sigma} c_{i\sigma} \rangle + \langle c_{j\sigma}^\dagger c_{j-\sigma} c_{i-\sigma}^\dagger c_{i\sigma} \rangle \right\}. \quad (16)$$

The local term can rigorously be expressed by the single-electron spectral density (6) although containing a “higher” expectation value [28]. It therefore allows for a selfconsistent determination within respective approaches to the fundamental spectral density. As soon as the “bandshift” $B_{-\sigma}$ gets a real spin-dependence it becomes decisive for the possibility of spontaneous ferromagnetism [29,30]. It shifts the centers of gravity of the quasiparticle subbands.

The second term $b_{\mathbf{k}-\sigma}$ in (15) consists of a density–density term, a double hopping and a spinflip correlation. Because of

$$\sum_{\mathbf{k}} b_{\mathbf{k}-\sigma} = 0, \quad (17)$$

it does not affect the center of gravity but the widths of the quasiparticle subbands, and that possibly in a different manner for different spin σ . (15) and (16) show that $B_{\mathbf{k}-\sigma} \rightarrow T_0$ in the $W \rightarrow 0$ limit so that (11)–(13) reproduce the the exact zero bandwidth limit (8).

In this paper we shall investigate the influence of magnetic order on the electrical conductivity of correlated band electrons. Since ferromagnetism is surely a strong-coupling phenomenon we restrict our considerations and the proposed approach accordingly. Since the rough structure of $S_{\mathbf{k}\sigma}(E)$ is known in the strong coupling regime, one could start with a corresponding ansatz for this fundamental function. If one assumes that quasiparticle damping is not decisive for ferromagnetism a two-pole ansatz suggests itself [29]:

$$S_{\mathbf{k}\sigma}(E) = \hbar \sum_{j=1}^2 \alpha_{j\sigma}(\mathbf{k}) \delta(E + \mu - E_{j\sigma}(\mathbf{k})). \quad (18)$$

The spectral weights $\alpha_{j\sigma}(\mathbf{k})$ and the quasiparticle energies $E_{j\sigma}(\mathbf{k})$ are fixed by equating the first four spectral moments,

$$M_{\mathbf{k}\sigma}^{(n)} = \frac{1}{\hbar} \int_{-\infty}^{\infty} dE E^n S_{\mathbf{k}\sigma}(E); \quad n = 0, \dots, 3, \quad (19)$$

which can be calculated rigorously and independently of the spectral density by use of the equivalent relation:

$$M_{\mathbf{k}\sigma}^{(n)} = \left\langle \left[\left(i\hbar \frac{\partial}{\partial t} \right)^n c_{\mathbf{k}\sigma}(t), c_{\mathbf{k}\sigma}^\dagger(t') \right]_+ \right\rangle_{t=t'}. \quad (20)$$

This completes the Spectral Density Approach (SDA) which leads to a self-energy with formally the same structure as that of the zero-bandwidth limit (10). The only but decisive difference is that the “free” center of gravity T_0 is replaced by the “higher” spin-dependent correlation function $B_{\mathbf{k}-\sigma}$ (14). In spite of its simple concept the SDA provides a convincing qualitative description of band ferromagnetism [28, 29, 31]. For later purposes we cite the explicit expressions for the spectral weights and the quasiparticle energies [29]:

$$E_{j\sigma}^{\text{SDA}}(\mathbf{k}) = \frac{1}{2} \left[\varepsilon(\mathbf{k}) + U + B_{\mathbf{k}-\sigma} + (-)^j \sqrt{(U + B_{\mathbf{k}-\sigma} - \varepsilon(\mathbf{k}))^2 + 4U \langle n_{-\sigma} \rangle (\varepsilon(\mathbf{k}) - B_{\mathbf{k}-\sigma})} \right], \quad (21)$$

$$\alpha_{1\sigma}^{\text{SDA}}(\mathbf{k}) = \frac{B_{\mathbf{k}-\sigma} + U(1 - \langle n_{-\sigma} \rangle) - E_{1\sigma}^{\text{SDA}}(\mathbf{k})}{E_{2\sigma}^{\text{SDA}} - E_{1\sigma}^{\text{SDA}}} = 1 - \alpha_{2\sigma}^{\text{SDA}}(\mathbf{k}). \quad (22)$$

It is easy to check that these results reproduce the correct strong coupling behavior (11)–(13). However, the neglect of quasiparticle damping will turn out to be a serious disadvantage for the application of the SDA concept to the electrical conductivity as can be seen in the next section. It will force us to think about an extension of the method (see Sec. 4).

3. Electrical conductivity

In general transport properties require the application of two-particle Green functions. According to the well-known Kubo formula [18] the electrical tensor conductivity, *e.g.*, is expressed by a current–current correlation function:

$$\sigma^{\alpha\beta}(E) = V \int_0^{(k_B T)^{-1}} d\lambda \int_0^\infty dt \left\langle j^\beta(0) j^\alpha(t + i\lambda\hbar) \right\rangle e^{\frac{i}{\hbar}(E + i0^+)t}. \quad (23)$$

α, β indicate Cartesian components. For the Hubbard model (1) this formula leads to a Green function of the type [9]:

$$\left\langle \left\langle c_{i\sigma}^\dagger c_{m\sigma}; c_{j\sigma'}^\dagger c_{n\sigma'} \right\rangle \right\rangle.$$

As mentioned at the end of the last section we are going to extend the SDA concept to account for a realistic inclusion of quasiparticle damping. This will be done by a “modified” alloy analogy [26] to the Hubbard model which is evaluated by use of the Coherent Potential Approximation (CPA) [25,32,33]. The electrical conductivity should therefore be evaluated within the same scheme. Velický has done the pioneering work [24] showing that the conductivity of (fictitious) alloys can be expressed in a simple form completely consistent with the CPA ansatz. The CPA attacks the single-electron resolvent $G = (E - H)^{-1}$, the operator form of (5). In the case of alloys only the configuration average $\langle G \rangle_c$ is important. The configuration average of the Kubo formula (23) can be traced back to the averaging of a direct product of two single-electron resolvents $\langle GG \rangle_c$. The idea of the Velický-theory is to use diagrams of the same order and of the same topology (“single site approximation”) for the evaluation of $\langle GG \rangle_c$ as applied in the CPA for $\langle G \rangle_c$. The range of validity of the approach to $\langle GG \rangle_c$ shall be equally broad as that of $\langle G \rangle_c$ in the CPA. When the “vertex corrections” $\Gamma^{(2)} = \langle GG \rangle_c - \langle G \rangle_c \langle G \rangle_c$ following from the Kubo formula for the electrical conductivity are treated in this internally consistent manner then they can be shown [24,33] to vanish identically as long as time inversion symmetry is satisfied:

$$\varepsilon(\mathbf{k}) = \varepsilon(-\mathbf{k}), \quad (24)$$

$$v_\alpha(\mathbf{k}) = \frac{1}{\hbar} \partial_{k_\alpha} \varepsilon(\mathbf{k}) = -v_\alpha(-\mathbf{k}). \quad (25)$$

The dc-conductivity $\sigma^{\alpha\beta}(E=0)$ of the (fictitious) alloy turns out to be expressible in terms of single-electron functions as, *e.g.*, the spectral density (6):

$$\sigma^{\alpha\beta} \sim \int dE \left(-f'_-(E) \right) \sum_{\mathbf{k}\sigma} v_\alpha(\mathbf{k}) v_\beta(\mathbf{k}) \left(S_{\mathbf{k}\sigma}(E - \mu) \right)^2. \quad (26)$$

$f'_-(E)$ is the derivative with respect to E of the Fermi function. The \mathbf{k} -independence of the CPA selfenergy [25] allows for an equivalent representation:

$$\begin{aligned} \sigma^{\alpha\beta} \sim & \sum_{\sigma} \int dE \left(-f'_-(E) \right) \int dx \left(\frac{I_\sigma(E)}{(E - x - R_\sigma(E))^2 + I_\sigma(E)} \right)^2 \\ & \times \sum_{\mathbf{k}} v_\alpha(\mathbf{k}) v_\beta(\mathbf{k}) \delta(x - \varepsilon(\mathbf{k})). \end{aligned} \quad (27)$$

Obviously the conductivity separates into two independent spin contributions. Eq. (27) permits a clear physical interpretation. The first part, the E integration, is due to the quantum statistics of the charge carriers (fermions).

The second part, the x -integral, depends on the dynamical properties of the system (1) being therefore most decisive. The third part, the \mathbf{k} -summation, refers to the bandstructure and therewith to the crystal structure. It is often called the “velocity function”. For a cubic crystal ($\sigma^{\alpha\beta} = 0$ if $\alpha \neq \beta$, $\sigma^{xx} = \sigma^{yy} = \sigma^{zz}$) its contribution to (27) reduces to:

$$v(x) = \frac{1}{N} \sum_{\mathbf{k}} \left(\frac{1}{\hbar} \nabla_{\mathbf{k}} \varepsilon(\mathbf{k}) \right)^2 \delta(x - \varepsilon(\mathbf{k})). \quad (28)$$

$v(x)$ represents a continuous and non-singular function of x being unequal zero just in that energy region where the “free” Bloch-Density Of States (B-DOS),

$$\rho_0(x) = \frac{1}{N} \sum_{\mathbf{k}} \delta(x - \varepsilon(\mathbf{k})), \quad (29)$$

is finite. For the cubic lattices $\nabla_{\mathbf{k}}^2 \varepsilon(\mathbf{k}) = -ca^2 \varepsilon(\mathbf{k})$ (a — lattice constant, $c_{\text{sc}} = 1$, $c_{\text{bcc}} = 3/4$, $c_{\text{fcc}} = 1/2$) so that (28) can be rewritten by using the method of partial integration [34]:

$$\frac{d}{dx} v(x) = -\frac{ca^2}{\hbar^2} x \rho_0(x). \quad (30)$$

From this we can justify the numerically useful representation of the velocity function:

$$v(x) = -\frac{ca^2}{\hbar^2} \int_{-\infty}^x d\epsilon \epsilon \rho_0(\epsilon). \quad (31)$$

The subsequent evaluation of our theory will be applied to bcc and fcc lattices. The corresponding B-DOS are plotted in Fig. 1(a). For testing reasons we also consider a simple symmetric triangular model DOS (full line in Fig. 1(a)). For a given B-DOS the velocity function (31) is easily calculated (see Fig. 1(b)). For the symmetric triangular B-DOS the dispersion relation $\varepsilon(\mathbf{k})$ is unknown. We, therefore, simply postulate that the velocity function in this case, too, is determined by the integral on the right-hand side of (31) together with an unimportant numerical pre-factor. The curves in Fig. 1(b) demonstrate that because of the integration $v(x)$ is more regular than $\rho_0(x)$. Eventually the conductivity (27) can be written for cubic lattices in the following form:

$$\sigma^{\alpha\alpha}(0) = \sigma_0 \sum_{\sigma} \int dE \left(-f'_{-}(E) \right) \int dx \phi(x, E) \hat{v}(x), \quad (32)$$

$$\phi(x, E) = \frac{I_{\sigma}^2(E)}{\left((E - x - R_{\sigma}(E))^2 + I_{\sigma}^2(E) \right)^2}, \quad (33)$$

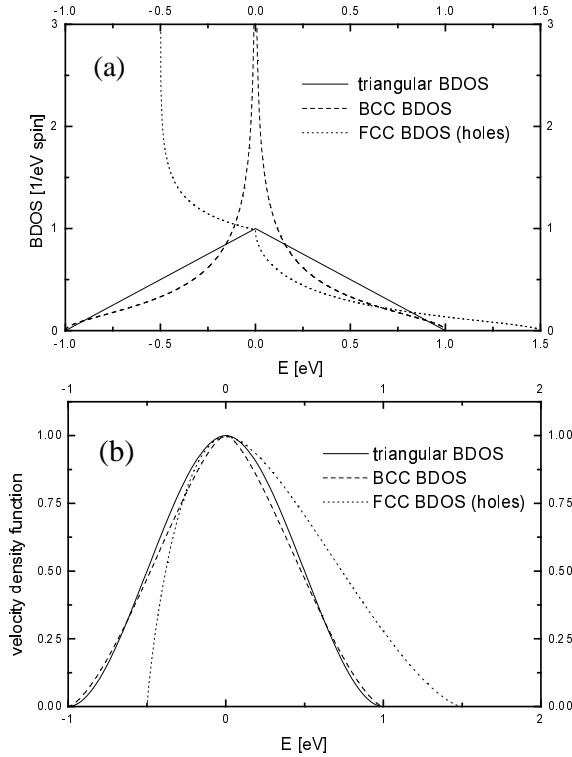


Fig. 1. (a) Bloch density of states ρ_0 as function of energy E for three different model systems: fcc lattice — dotted line; bcc lattice — broken line; fictitious test system — full line. (b) Normalized velocity function v as function of energy E for the three “free” B-DOS of part (a).

$$\hat{v}(x) = - \int_{-\infty}^x d\epsilon \epsilon \rho(\epsilon). \quad (34)$$

The numerical factor σ_0 gathers all the constants. If the imaginary part of the selfenergy is rather small and a smooth function of E in the region around the chemical potential μ where $f'_-(E)$ is unequal zero, then we can replace in good approximation:

$$\begin{aligned} \phi(x, E) &\longrightarrow \frac{-I_\sigma(E)}{(E - x - R_\sigma(E))^2 + I_\sigma^2(E)} \pi \delta(E - x - R_\sigma(E)) \\ &= \frac{-\pi}{I_\sigma(E)} \delta(E - x - R_\sigma(E)). \end{aligned} \quad (35)$$

That means for the conductivity expression:

$$\sigma^{\alpha\alpha}(0) = -\pi\sigma_0 \sum_{\sigma} \int dE \left(-f'_{-}(E) \right) \frac{\hat{v}(E - R_{\sigma}(E))}{I_{\sigma}(E)}. \quad (36)$$

At $T = 0$ K the derivative $f'_{-}(E)$ becomes a δ -function at $\mu(T = 0) = E_{\text{F}}$ and $\sigma^{\alpha\alpha}(0)$ simplifies further to:

$$\sigma^{\alpha\alpha}(0) \approx -\pi\sigma_0 \sum_{\sigma} \frac{\hat{v}(E_{\text{F}} - R_{\sigma}(E_{\text{F}}))}{I_{\sigma}(E_{\text{F}})}. \quad (37)$$

Vanishing imaginary part of the selfenergy at the Fermi energy (Fermi liquid) leads to a diverging conductivity.

4. Modified alloy analogy

The dc-conductivity (32) is known as soon as we have found the electronic selfenergy (4). According to the simplifications (36) and (37) in particular the imaginary part plays a decisive role. One of the first and best known approaches to the Hubbard model that includes quasiparticle damping, and therewith a complex selfenergy, uses an alloy analogy as proposed by Hubbard himself [21]. If one assumes for the moment that the $(-\sigma)$ -electrons are frozen at certain lattice sites then a propagating σ -electron encounters an effective binary alloy. At empty lattice sites it finds the atomic energy $E_{1\sigma}$, at sites with a $(-\sigma)$ -electron present the atomic energy $E_{2\sigma}$. The two levels are randomly distributed over the lattice with “concentrations” $x_{1\sigma}$ and $x_{2\sigma}$ corresponding to the respective probabilities for the σ -electron to meet the one or the other situation. In the conventional alloy analogy the energies $E_{p\sigma}$ and the “concentrations” $x_{p\sigma}$ are taken from the zero-bandwidth limit (8):

$$E_{1\sigma}^{\text{AA}} = T_0; \quad E_{2\sigma}^{\text{AA}} = T_0 + U, \quad (38)$$

$$x_{1\sigma}^{\text{AA}} = 1 - \langle n_{-\sigma} \rangle; \quad x_{2\sigma}^{\text{AA}} = \langle n_{-\sigma} \rangle. \quad (39)$$

A standard method for solving such alloy problems is the CPA [24, 25, 32]. It represents a single-site approximation leading therewith to a \mathbf{k} -independent selfenergy $\Sigma_{\mathbf{k}\sigma}(E) \equiv \Sigma_{\sigma}(E)$ which solves the following equation:

$$0 = \sum_{p=1}^2 x_{p\sigma} \frac{E_{p\sigma} - \Sigma_{\sigma}(E) - T_0}{1 - \frac{1}{\hbar} G_{\sigma}(E) [E_{p\sigma} - \Sigma_{\sigma}(E) - T_0]}. \quad (40)$$

$$G_{\sigma}(E) = \frac{1}{N} \sum_{\mathbf{k}} G_{\mathbf{k}\sigma}(E), \quad (41)$$

T_0 is the center of gravity of the Bloch dispersion $\varepsilon(\mathbf{k})$. It has to be included in (40) to ensure the correct behavior in the zero bandwidth limit $W = 0$. The solution of (40) yields a selfenergy with a non-zero imaginary part in certain energy regions. However, spontaneous ferromagnetism is excluded, in remarkable contradiction to the SDA results [29]. On the other hand, the CPA has gained strong support by the recently proven fact [35] that it is an exact treatment of the alloy problem in infinite lattice dimensions. The CPA solution for the alloy analogy (38), (39), however, does not reproduce the correct strong coupling behavior ((11)–(13)) of the Hubbard model. This discrepancy can be explained only by the conclusion that the underlying alloy analogy (38), (39) must be wrong. In particular, the assumption of frozen ($-\sigma$)-electrons is surely not acceptable.

The CPA theory allows exact analytical statements in the “split band regime”, where the atomic levels of the alloy constituents are far away from each other. Within the alloy analogy this corresponds to the strong coupling regime ($W \ll U$) of the Hubbard model. In this regime the CPA predicts a spectral density $S_{\mathbf{k}\sigma}(E)$ which consists of two well-separated peaks. The detailed shapes of the peaks are not known but their centers of gravity:

$$T_{pj\sigma}^{\text{CPA}}(\mathbf{k}) \longrightarrow E_{j\sigma} + x_{j\sigma}(\varepsilon(\mathbf{k}) - T_0). \quad (42)$$

The peak areas coincide with the concentrations $x_{j\sigma}$. By comparing these exact CPA results with the respective strong coupling results (11)–(13) we come to new atomic levels $E_{j\sigma}$ and “concentrations” $x_{j\sigma}$. The comparison makes sense, of course, only if the single-site aspect of the CPA is accounted for in (12) and (13), too. This requires the suppression of the “bandwidth correction” $b_{\mathbf{k}-\sigma}$ (16). The “modified” alloy analogy turns out to be expressible by the SDA results (21) and (22) in the strong coupling limit ($U/W \gg 1$):

$$E_{j\sigma} = \left(\left(E_{j\sigma}^{\text{SDA}}(\mathbf{k}) \right)_{U/W \gg 1} \right)_{\varepsilon(\mathbf{k}) \rightarrow T_0}, \quad (43)$$

$$x_{j\sigma} = \left(\left(\alpha_{j\sigma}^{\text{SDA}}(\mathbf{k}) \right)_{U/W \gg 1} \right)_{\varepsilon(\mathbf{k}) \rightarrow T_0}. \quad (44)$$

By extending these considerations, which are justified for the strongly coupled Hubbard model, in an obvious way to moderate couplings,

$$E_{j\sigma}^{\text{MAA}} = \left(E_{j\sigma}^{\text{SDA}}(\mathbf{k}) \right)_{\varepsilon(\mathbf{k}) \rightarrow T_0}, \quad (45)$$

$$x_{j\sigma}^{\text{MAA}} = \left(\alpha_{j\sigma}^{\text{SDA}}(\mathbf{k}) \right)_{\varepsilon(\mathbf{k}) \rightarrow T_0}. \quad (46)$$

a Modified Alloy Analogy (MAA) is created. The energy levels $E_{j\sigma}^{\text{MAA}}$ and the concentrations $x_{j\sigma}^{\text{MAA}}$ are given by the SDA results (21) and (22), when the “free” energies $\varepsilon(\mathbf{k})$ are replaced by the center of gravity T_0 . Note that this also implies $B_{\mathbf{k}-\sigma} \rightarrow B_{-\sigma}$, because the bandwidth correction $b_{\mathbf{k}-\sigma}$ (16) vanishes for $\varepsilon(\mathbf{k}) \rightarrow T_0$ (see Eq. (26) in Ref. [29]).

In the Modified Alloy Analogy the energy levels and concentrations are not only dependent on the model parameters T_0 and U but also on the occupation number $\langle n_{-\sigma} \rangle$ and the bandshift $B_{-\sigma}$. Both have to be determined selfconsistently, $\langle n_{-\sigma} \rangle$ via (9) and $B_{-\sigma}$ by use of [26, 28, 36]:

$$\langle n_{-\sigma} \rangle (1 - \langle n_{-\sigma} \rangle) (B_{-\sigma} - T_0) = \frac{1}{\hbar} \text{Im} \int_{-\infty}^{+\infty} dE f_{-}(E) \left(\frac{2}{U} \Sigma_{-\sigma}(E - \mu) - 1 \right) \times [(E - \Sigma_{-\sigma}(E - \mu) - T_0) G_{-\sigma}(E - \mu) - \hbar]. \quad (47)$$

In the strict zero-bandwidth limit $B_{-\sigma}$ is identical to T_0 and the conventional alloy analogy (38), (39) is reproduced. As soon as the hopping is switched on, however, $B_{-\sigma}$ deviates from T_0 and the type of the underlying alloy changes in each step of the iteration process. The atomic levels $E_{j\sigma}^{\text{MAA}}$ possibly get real spin-dependencies. It can be demonstrated [26] that the itineracy of the $(-\sigma)$ -electrons comes indirectly via $B_{-\sigma}$ into play, removing therewith a shortcoming of the conventional alloy analogy. When we insert the “modified” alloy data (45), (46) into the CPA equation (40) we find a solution strongly related to the SDA (Sec. 2) but now with the inclusion of quasiparticle damping. The strong coupling behavior is exactly reproduced. In Ref. [37] the MAA is additionally justified and confirmed from the rigorous high-energy expansion of the propagator $G_{\sigma}(E)$ and the selfenergy $\Sigma_{\sigma}(E)$ in (40) by equating exactly calculated spectral moments (20).

5. Magnetic order and electrical conductivity

Contrary to the conventional alloy analogy of the Hubbard model the MAA predicts ferromagnetism in restricted parameter regions. Fig. 2 shows as an example the spectral density $S_{\mathbf{k}\sigma}(E)$ of a strongly correlated ($U/W=5$) electron system on an fcc lattice. As B-DOS (29) a tight-binding version [38] has been chosen. For less than half-filled bands ($n < 1$) the system is paramagnetic, no spontaneous spin order appears. The band occupation $n = 1.6$ in Fig. 2, however, allows band ferromagnetism provided the Coulomb interaction U exceeds a critical value. Two types of splitting occur. At first the spectral density consists, for each \mathbf{k} -vector, of a high-energy and a low-energy peak separated by an energy of the order U . The finite widths of the peaks are due to quasiparticle damping. The weight (area) of the

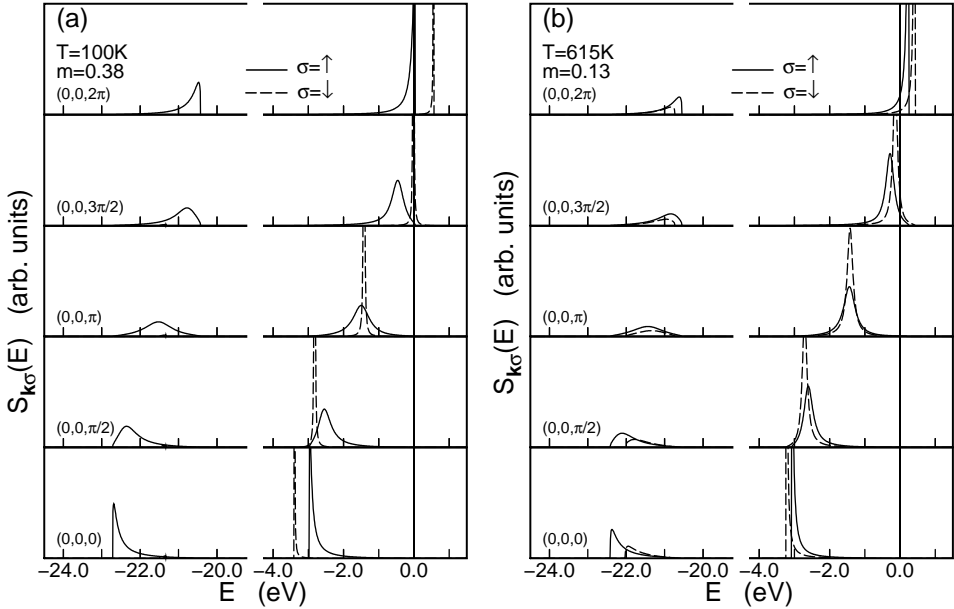


Fig. 2. Spectral density as a function of energy for an fcc lattice calculated within the MAA. (a) $T = 100$ K, (b) $T = 615$ K. \mathbf{k} -vectors equidistant along the $(0,0,1)$ direction of the 1. Brillouin zone. Further parameters: $n = 1.6$, $U = 20$ eV, $W = 4$ eV.

lower peak refers to the probability that the propagating (\mathbf{k}, σ) -electron in the more than half-filled band enters an empty site, while the weight of the upper peak scales with the probability that the (\mathbf{k}, σ) -electron meets a $(-\sigma)$ -electron. This splitting appears for all temperatures. Ferromagnetism arises when these two spectral density peaks exhibit an additional spin splitting. At low temperatures ($T = 100$ K in Fig. 2(a)) the system is very close to its saturation ($m = 2 - n$), *i.e.*, the up-spin states are almost fully occupied. A down-spin electron cannot avoid to meet an up-spin electron at every lattice site and has to perform a Coulomb interaction. Consequently the low-energy peak of $S_{\mathbf{k}\downarrow}(E)$ disappears. At higher temperatures (Fig. 2(b)) the peak reappears because of a partial demagnetization of the electron system. At low temperatures the high-energy peaks of $S_{\mathbf{k}\downarrow}(E)$ are very sharp, indicating long-living quasiparticles. An interesting \mathbf{k} -dependence of the peak position (quasiparticle energy) is observed in the region around the chemical potential μ . At the top of the dispersion a “normal” exchange splitting appears, *i.e.*, the \downarrow -peak is located above the \uparrow -peak. At the bottom of the dispersion, however, the \uparrow -energy is higher than the respective \downarrow -energy (“inverse exchange splitting”). The quasiparticle dispersions of the two spin parts are crossing as functions of the wave-vector \mathbf{k} .

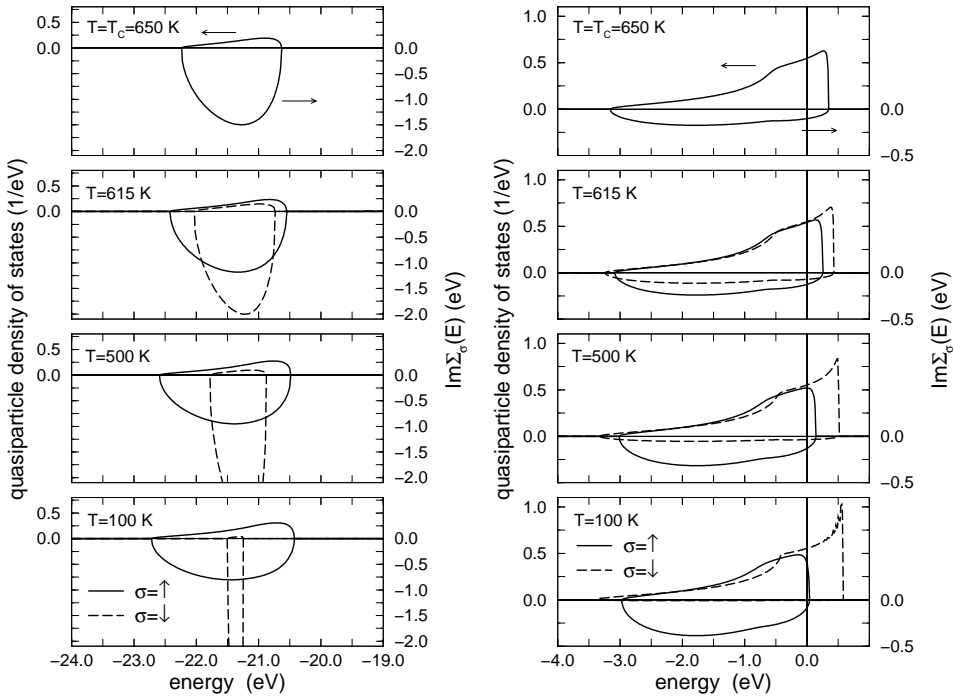


Fig. 3. Quasiparticle density of states ρ_σ (upper half) and imaginary part of the selfenergy I_σ (lower half) as function of energy and different temperatures up to T_C . Left part for the lower subband, right part for the upper subband. The chemical potential μ marks the energy zero. Other parameters as in Fig. 2

This behavior is due to two competing correlation effects, a spin-dependent exchange shift of the centers of gravity of the quasiparticle spectra and a spin-dependent band narrowing.

According to (7) a wave-vector summation of the spectral density yields the Quasiparticle Density Of States (QDOS). For the same model parameters as in Fig. 2 the temperature-dependent QDOS is plotted in Fig. 3. The two types of splitting of the spectral density (Fig. 2) cause respective splittings of the QDOS. The spin-splitting of each of the two ‘‘Hubbard bands’’ creates the critical temperature T_C . With decreasing temperature an increasing spin asymmetry appears. For low temperatures ($T = 100$ K in Fig. 3) the MAA predicts an almost saturated ferromagnetism. The \uparrow -states are practically all occupied. The lower \downarrow -subband therefore disappears because a \downarrow -electron has no chance to find an empty lattice site. Since each site is occupied by one \uparrow -electron no scattering processes happen for the \downarrow -electrons. The upper \downarrow -subband has therefore at low temperatures the shape of the ‘‘free’’ fcc B-DOS (Fig.1(a)). The imaginary part $I_\sigma(E)$ of the selfenergy, also shown

in Fig. 3, is a measure for quasiparticle damping. Consequently $I_{\downarrow}(E)$ vanishes for $T \rightarrow 0$. With increasing temperature (increasing demagnetization) quasiparticle damping is enhanced, accompanied by a growing up of the imaginary part of the selfenergy. The shape of the QDOS more and more deviates from that of the B-DOS. The behavior of $I_{\sigma}(E)$ decisively influences the dc-conductivity (32).

Within the MAA the fcc Hubbard model shows ferromagnetism only for more than half-filled bands. The bandoccupation dependence of T_C is plotted in Fig. 4 for very strongly correlated band electrons ($U/W = 5$ and $U/W = 12.5$). For these couplings ferromagnetism is possible in the whole region $1 < n < 2$. For $n \geq 1.5$ the phase transitions are of second order changing to first order transitions for $1 < n < 1.5$. It is not clear to us whether the first order transitions are artifacts of the MAA or true characteristics of

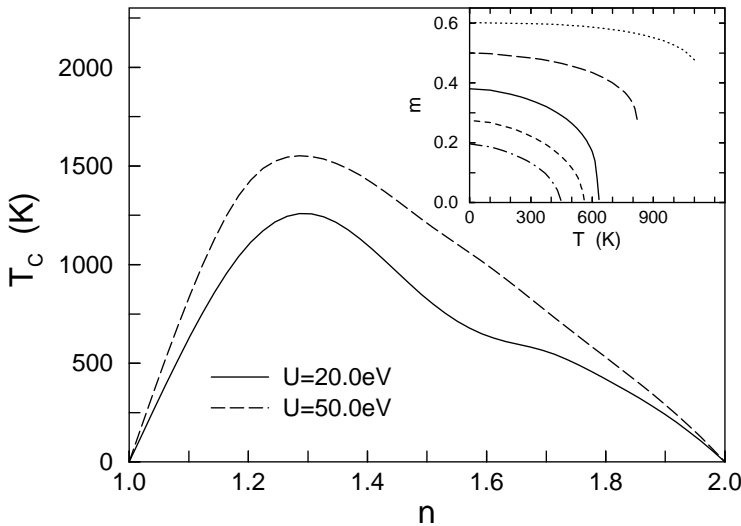


Fig. 4. Curie temperature T_C as a function of band occupation n for two different values of U . The inset shows the magnetization m as a function of temperature T for various band occupations n (dashed-dotted line — $n = 1.8$; dashed line — $n = 1.7$; solid line — $n = 1.6$; long-dashed line — $n = 1.5$; dotted line — $n = 1.4$). Further parameters: fcc B-DOS, $W = 4$ eV.

the Hubbard model. The U -dependence of T_C for fixed bandoccupation n can be described as follows: U must exceed a critical value U_c to allow for a spontaneous ferromagnetic order. With increasing U the Curie temperature T_C steeply shifts to higher values running very soon, however, into a saturation. U_c as well as the saturation value are different for different band occupations.

Let us now discuss the influence of magnetic order on the dc-conductivity (32). Fig. 5 shows the band occupation dependence of the conductivity at $T = 0\text{K}$ for three different \mathbf{k} -values, and that for a paramagnetic electron system. Paramagnetism is always a mathematical solution within the MAA scheme. We disregard in Fig. 5 that additional ferromagnetic solutions,

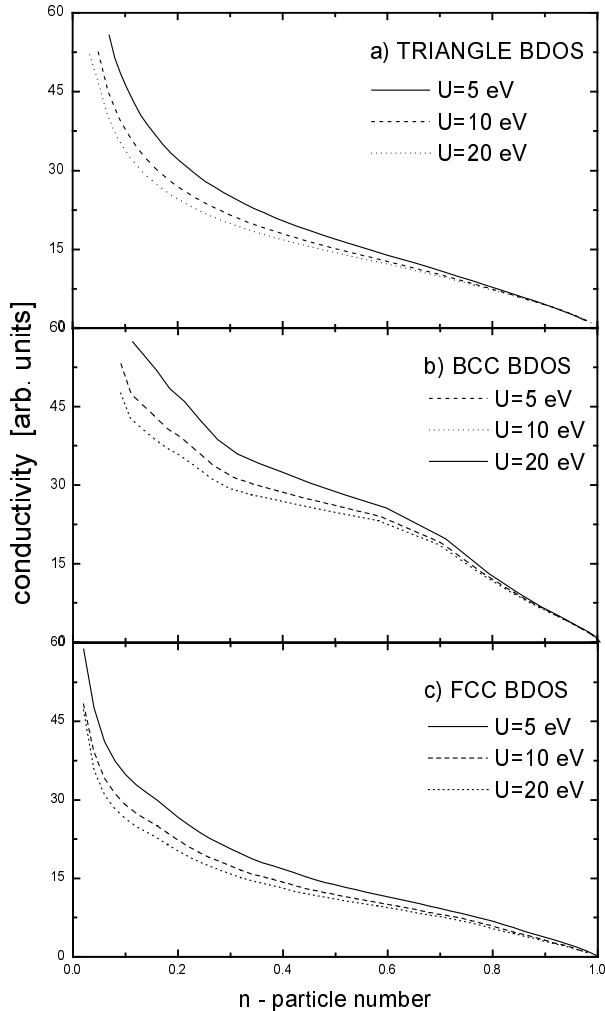


Fig. 5. Total electrical conductivity as function of particle density n in the paramagnetic state at high temperature for three different Coulomb interactions U (solid line — $U = 5\text{ eV}$; dashed line — $U = 10\text{ eV}$; dotted line — $U = 20\text{ eV}$). (a) fictitious triangle B-DOS, (b) bcc, (c) fcc.

if they exist, are always more stable than the paramagnetic one. For the triangular B-DOS (Fig. 5(a)) ferromagnetism does not appear at all. The bcc lattice exhibits in a small region of n and for a sufficiently high U ferromagnetic order [26], while the fcc lattice orders ferromagnetically for all band occupations above half-filling (Fig. 4). All the curves in Fig. 5 concern the paramagnetic solution. In any case the conductivity $\sigma^{\alpha\alpha}(0)$ turns out to be a continuously decreasing function of the carrier concentration n disappearing for $n = 1$. Because of the strong coupling splitting of the Bloch band into two quasiparticle subbands (Hubbard bands) (Fig. 3) the system is insulating for $n = 1$ (Mott insulator). The lower subbands are fully occupied, the upper subbands are empty. The divergence of $\sigma^{\alpha\alpha}(0)$ for $n \rightarrow 0$ reflects the situation of charge carriers freely moving in the periodic lattice without any scattering. The conductivity curves for different lattice structures are very similar. They show a slight decrease with increasing Coulomb coupling U .

The ferromagnetic order drastically influences the conductivity behavior. Spin up and spin down channels contribute additively to the total conductivity in the considered electron system [24]. In the ferromagnetic phase the conductivity of \uparrow -electrons is strongly enhanced compared to the paramagnetic case, while that of \downarrow -electrons is suppressed. According to formula (36) the imaginary part of the selfenergy $I_{\sigma}(E)$ in the thin stripe around μ ($\Delta \approx 4k_B T$), where $f'_{\downarrow}(E)$ is finite, determines the conductivity. For the less than half-filled band $|I_{\downarrow}(E)| > |I_{\uparrow}(E)|$ is found [26]. Near the chemical potential \downarrow -electrons are substantially stronger damped than \uparrow -electrons. This results in a higher contribution of the \uparrow -electrons to the conductivity.

Fig. 6 shows the temperature dependence of the conductivity in the fcc lattice for band occupations $1 < n < 2$. The dominating contribution to the conductivity in the ferromagnetic phase comes from the \downarrow -electrons. Again the explanation is the imaginary part of the selfenergy in Eq. (36), which according to Fig. 3 is at low temperatures very much smaller for \downarrow than \uparrow . For $T \rightarrow 0$ the magnetic moment is almost saturated, the \uparrow -states are occupied. Therefore $\sigma^{\alpha\alpha}(0)$ disappears for \uparrow -electrons at very low temperatures. With increasing temperature ($T \lesssim T_C$) the \downarrow -conductivity strongly decreases and the \uparrow -conductivity slightly increases to coincide at T_C . The first order transition for $n = 1.4$ manifests itself in a corresponding jump of the conductivity at T_C . The electrical resistivity (Fig. 6(b)) disappears in the ferromagnetic phase for $T \rightarrow 0$. The current is then build up exclusively by \downarrow -electrons which do not scatter within the framework of the Hubbard model (1).

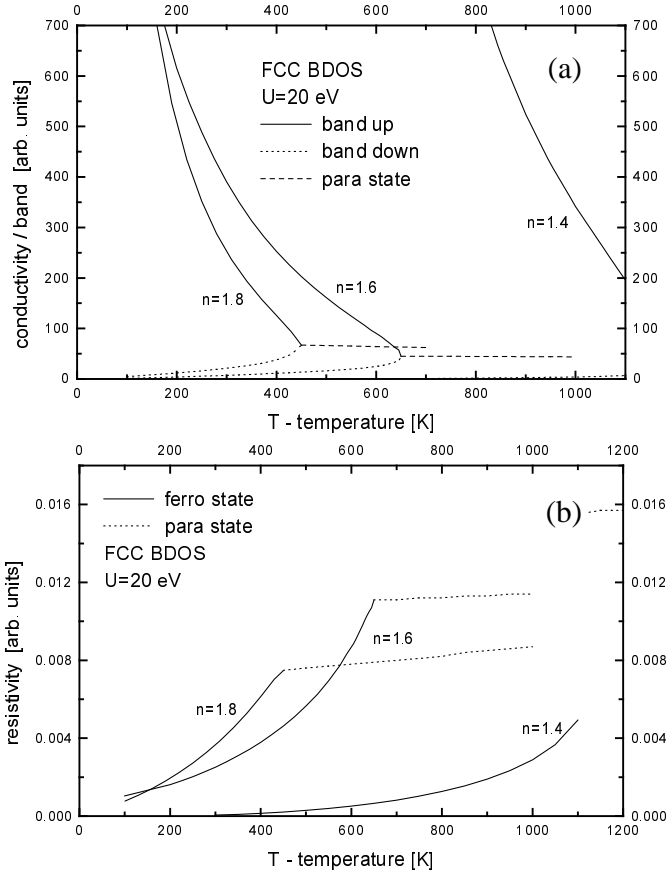


Fig. 6. Electrical conductivity as function of temperature for three different band occupations n in an fcc lattice (B-DOS as in Fig. 1(a)). $U = 20$ eV, $W = 4$ eV. Full line — $\sigma = \uparrow$; dotted line — $\sigma = \downarrow$; dashed line — $\sigma = \uparrow, \downarrow$ (paramagnetic phase). Note the first order transition at T_C for $n = 1.4$. (b) Total electrical resistivity as function of temperature calculated for the same parameters as in (a).

6. Conclusions

We have developed for the single-band Hubbard model a Modified Alloy Analogy (MAA) which we solved by use of CPA. The main goal is to investigate the possibility of ferromagnetism in the Hubbard model and the influence of quasiparticle damping on the stability of the magnetic state. The atomic levels and the concentrations of the constituents of the fictitious alloy are found by fitting the exact strong coupling regime of the Hubbard model. The results differ from the “normal” alloy analogy which refers to the zero-bandwidth limit. In the MAA atomic levels and concentration con-

tain certain (spin-dependent) expectation values which depend on the model parameters (Bloch band width, band occupation, temperature, ...). That means that the character of the alloy alters at each step of the iteration process therewith accounting for the itineracy of ($-\sigma$)-electrons when the σ -electron is propagating through the alloy. The MAA yields ferromagnetism in the Hubbard model for the non-bipartite fcc lattice in the case of a more than half-filled energy band ($1 < n < 2$) and also for the bcc lattice, but in a rather restricted region of the particle density n . Additionally the Coulomb interaction U must exceed a critical value.

We have used the CPA consistent theory of Velický [24] to discuss the electrical conductivity of the Hubbard model and its interplay with the spontaneous magnetic order. Because of vanishing vertex corrections the conductivity is expressed by the real and imaginary part of the electronic selfenergy. The latter are found by use of the MAA. In the ferromagnetic phase the conductivity is substantially higher than in the paramagnetic one, and is mainly due to the majority-spin carriers. In the ferromagnetic saturation, where electron-electron scattering cannot happen, the imaginary part of the selfenergy vanishes giving rise to a diverging conductivity for $T \rightarrow 0$. The electrical resistivity exhibits a power-like temperature behavior at low temperatures (it was established numerically that $\rho \sim T^\alpha$ with α close to 3) becoming critical at T_C . The temperature curves for the conductivity and the resistivity, respectively, are qualitatively very similar to those of metallic rare earth elements and their alloys, for which an exchange interaction between itinerant band electrons and localized (magnetic) 4f electrons dominates the physical properties ("spin disorder resistivity") [39–41]. The present theory discusses exclusively the effect of electron–electron scattering on the electrical conductivity; phonon and impurity contributions are not taken into account.

This work has been done within the Sonderforschungsbereich 290 "Metalliche dünne Filme: Struktur, Magnetismus und elektronische Eigenschaften" of the Deutsche Forschungsgemeinschaft and the Polish State Committee for Scientific Research (KBN) project number P03B 129 14.

REFERENCES

- [1] J. Hubbard, *Proc. R. Soc. Lond., A Math. Phys. Sci.* **276**, 238 (1963).
- [2] J. Hubbard, *Proc. R. Soc. Lond., A Math. Phys. Sci.* **277**, 237 (1964).
- [3] J. Hubbard, *Proc. R. Soc. Lond., A Math. Phys. Sci.* **281**, 401 (1964).
- [4] R.A. Bari, D. Adler, R.V. Lange, *Phys. Rev.* **B2**, 2898 (1970).
- [5] R.A. Bari, T.A. Kaplan, *Phys. Rev.* **B6**, 4623 (1972).

- [6] U. Brandt, W. Gross, *Z. Phys.* **263**, 69 (1973).
- [7] M. Eswaran, J.C. Kimball, *Phys. Rev.* **B11**, 3420 (1975).
- [8] W. Schiller, G. Röpke, V. Christoph, *Phys. Status Solidi* **B72**, K49 (1975).
- [9] W. Nolting, *Phys. Status Solidi* **B70**, 505 (1975).
- [10] E. Marsch, *J. Phys. C* **9**, L117 (1976).
- [11] E.N. Economou, P. Mihas, *J. Phys. C* **10**, 5017 (1977).
- [12] R.R. DeMarco, E.N. Economou, C.T. White, *Phys. Rev.* **B18**, 3968 (1978).
- [13] S.H. Liu, *Phys. Rev.* **B15**, 4281 (1977).
- [14] W. Schumacher, *Phys. Status Solidi* **B120**, 621 (1983).
- [15] M. Kaveh, N. Wisser, *Adv. Phys.* **33**, 257 (1984).
- [16] V.I. Grebennikov, Yu.I. Prokopjev, *Sov. Phys. Metal. Metalloved.* **60**, 213 (1985).
- [17] K. Kubo, *J. Phys. Soc. Jpn.* **31**, 30 (1972).
- [18] R. Kubo, *J. Phys. Soc. Jpn.* **12**, 570 (1957).
- [19] K.A. Kikoin, V.N. Flerov, *Sov. Phys. – Solid State* **16**, 237 (1974).
- [20] W. Metzner, D. Vollhardt, *Phys. Rev. Lett.* **62**, 324 (1989).
- [21] D. Vollhardt, *Correlated Electron Systems*, Ed. V.J. Emery, World Scientific, Singapore 1993, p. 57.
- [22] A. Georges, G. Kotliar, *Phys. Rev.* **B45**, 6479 (1992).
- [23] M. Jarrell, *Phys. Rev. Lett.* **69**, 168 (1992).
- [24] B. Velický, *Phys. Rev.* **184**, 614 (1969).
- [25] B. Velický, S. Kirkpatrick, H. Ehrenreich, *Phys. Rev.* **175**, 747 (1968).
- [26] T. Herrmann, W. Nolting, *Phys. Rev.* **B53**, 10579 (1996).
- [27] A.B. Harris, R.V. Lange, *Phys. Rev.* **157**, 295 (1967).
- [28] G. Geipel, W. Nolting, *Phys. Rev.* **B38**, 2608 (1988).
- [29] T. Herrmann, W. Nolting, *J. Magn. Magn. Mater.* **170**, 253 (1997).
- [30] M. Potthoff, T. Herrmann, T. Wegner, W. Nolting, preprint.
- [31] T. Herrmann, W. Nolting, *Solid State Commun.* **103**, 351 (1997).
- [32] R.J. Elliott, J.A. Krumhansl, P.L. Leath, *Rev. Mod. Phys.* **46**, 465 (1974).
- [33] F. Yonezawa, K. Morigaki, *Suppl. Progr. Theor. Phys.* **53**, 1 (1973).
- [34] K. Hoshino, K. Niizeki, *J. Phys. Soc. Jpn.* **38**, 1320 (1975).
- [35] R. Vlammig, D. Vollhardt, *Phys. Rev.* **B45**, 4637 (1992).
- [36] M. Potthoff, W. Nolting, *J. Phys. Condens. Matter* **8**, 4937 (1996).
- [37] M. Potthoff, T. Herrmann, W. Nolting, in print.
- [38] R.J. Jelitto, *J. Phys. Chem. Solids* **30**, 609 (1969).
- [39] T. van Peski-Tinbergen, A.J. Dekker, *Physica* **29**, 917 (1963).
- [40] S.H. Liu, *Phys. Rev.* **139**, 542 (1963).
- [41] W. Borgiel, W. Nolting, G. Borstel, *Z. Phys.* **B67**, 349 (1987).